



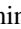



Experimental study of the Γ_{p1}/Γ_{p0} ratios of resonance states in ${}^8\text{Be}$ for deducing the ${}^7\text{Be}(n, p_1){}^7\text{Li}^*$ reaction rate relevant to the cosmological lithium problem

N. Iwasa ^{1,*}, S. Ishikawa,¹ S. Kubono ^{2,3}, T. Sakakibara,¹ K. Kominato,¹ K. Nishio ⁴, M. Matsuda,⁴ K. Hirose,⁴ H. Makii ⁴, R. Orlandi,⁴ K. Asada,¹ D. Guru,¹ S. Nishimura ², S. Hayakawa,³ and T. Kawabata ⁵

¹Department of Physics, Tohoku University, 6-3, Aramaki-aza-aoba, Aoba, Sendai, Miyagi 980-8578, Japan

²RIKEN Nishina Center, RIKEN, 2-1, Hirosawa, Wako, Saitama 351-0198, Japan

³Center for Nuclear Study (CNS), the University of Tokyo, RIKEN campus, 2-1 Hirosawa, Wako, Saitama 351-0198, Japan

⁴Advanced Science Research Center, Japan Atomic Energy Agency (JAEA), Tokai, Ibaraki 319-1195, Japan

⁵Department of Physics, Osaka University, 1-1 Machikaneyama, Toyonaka, Osaka 560-0043, Japan



(Received 23 September 2020; accepted 14 December 2020; published 6 January 2021)

The ${}^9\text{Be}({}^3\text{He}, \alpha){}^8\text{Be}^*(p){}^7\text{Li}$ reaction was studied at $E_{\text{lab}}({}^3\text{He}) = 30$ MeV to deduce the branching ratios of Γ_{p1}/Γ_{p0} of resonant states at 18.91–20.1 MeV in ${}^8\text{Be}$, which are necessary to extract the ${}^7\text{Be}(n, p_1){}^7\text{Li}^*$ reaction rate relevant to the ${}^7\text{Be}$ destruction in the big bang nucleosynthesis, from the ${}^7\text{Li}(p, n_0){}^7\text{Be}$ reaction cross section. The decay protons from ${}^8\text{Be}^*$ to the ground and first excited states in ${}^7\text{Li}$ were well-separately measured. The Γ_{p1}/Γ_{p0} ratio of the 19.235-MeV state was deduced to be $3.4 \pm 1.9\%$. The 19.86- and 20.1-MeV states were found to decay dominantly into the first excited and ground states of ${}^7\text{Li}$, respectively.

DOI: [10.1103/PhysRevC.103.015801](https://doi.org/10.1103/PhysRevC.103.015801)

I. INTRODUCTION

The big bang model is supported by the observations: the expansion of the Universe, the cosmic microwave background, and the big bang nucleosynthesis (BBN). The primordial abundances of ${}^2\text{H}$ and ${}^3,{}^4\text{He}$ are well reproduced by the standard BBN model using the “baryon density” parameter determined by the observation of the anisotropy of the cosmic microwave background. On the other hand, the primordial abundance of ${}^7\text{Li}$ is overestimated by a factor of three to four. This discrepancy is called “the cosmological lithium problem” [1]. Many theoretical and experimental studies were performed to solve the problem, but no solutions were found without using new physics beyond the standard model which was not confirmed experimentally [1].

The primordial ${}^7\text{Li}$ was mainly produced by the electron capture of ${}^7\text{Be}$ synthesized by the ${}^3\text{He}(\alpha, \gamma){}^7\text{Be}$ reaction. Although ${}^7\text{Li}$ was produced by the ${}^3\text{H}(\alpha, \gamma){}^7\text{Li}$ and ${}^7\text{Be}(n, p){}^7\text{Li}$ reactions in BBN, most of the ${}^7\text{Li}$ was immediately destroyed by the ${}^7\text{Li}(p, \alpha){}^4\text{He}$ reaction. Uncertainty on the ${}^7\text{Be}$ production rate is very small, because precise measurements of the ${}^3\text{He}(\alpha, \gamma){}^7\text{Be}$ reaction were reported by several groups [2]. If the destruction rate of ${}^7\text{Be}$ was large enough to reduce the primordial abundance of ${}^7\text{Li}$, then the present model would be validated without introducing any new physics.

The ${}^7\text{Be}(n, p){}^7\text{Li}$ reaction is thus the most important ${}^7\text{Be}$ destruction reaction in BBN. Its reaction rate used in the BBN model was compiled by Descouvemont *et al.* [3] using the ${}^7\text{Be}(n, p){}^7\text{Li}$ reaction cross sections directly measured by Koehler *et al.* at the neutron energy $E_n \leq 13.7$ keV [4]

and those deduced by measurements of the time-reversal reaction ${}^7\text{Li}(p, n){}^7\text{Be}$ [5–8]. The direct measurements of the ${}^7\text{Be}(n, p){}^7\text{Li}$ reaction by Hanna *et al.* [9], Gledenove *et al.* [10], and Cervena *et al.* [11] were not used in the compilation, but they are consistent with the results of Ref. [4] within their error.

The direct measurement of the ${}^7\text{Be}(n, p){}^7\text{Li}$ reaction cross section at $E_n \leq 325$ keV was reported by Damone *et al.* [12]. The cross section at low energies was 35–40% higher than that of Koehler *et al.* [4]. Since the cross section at high energies was less accurate than that reported by the time-reversal reaction measurements, the ${}^7\text{Be}(n, p_0){}^7\text{Li}$ cross section from the time-reversal reaction [7] at $E_n > 35$ keV was used for the reaction rate calculation, resulting in a 10% decrease of the predicted cosmological abundance of ${}^7\text{Li}$.

The ${}^7\text{Be}(n, p_1){}^7\text{Li}^*$ (0.478 keV; $\frac{1}{2}^-$) reaction is also ${}^7\text{Be}$ destruction reaction, but it was not studied well. The ratio of the ${}^7\text{Be}(n, p_1){}^7\text{Li}^*$ cross section to the ${}^7\text{Be}(n, p_0){}^7\text{Li}$ one, $\sigma_{np1}/\sigma_{np0}$, was measured to be $1.18 \pm 0.05\%$ (weighted mean value) for $E_n \leq 60$ eV and $3.2 \pm 1.2\%$ at $E_n = 60$ eV by Koehler *et al.* [4] and $1.2 \pm 0.6\%$ at thermal energy by Tomandl *et al.* [13]. They are lower than the resonant energy $E_n = 13$ keV for the 2_1^- state at 18.91 MeV in ${}^8\text{Be}$, which is the lowest known resonant state above the neutron separation energy $S_n = 18.899$ MeV. Although the (n, p_1) reaction was not separated from the (n, p_0) reaction around the 2_1^- state, the (n, p_1) reaction was also measured by the direct method. On the other hand, the (n, p_1) cross section cannot be deduced from the time-reversal reaction measurements. Therefore the ${}^7\text{Be}(n, p_1){}^7\text{Li}^*$ reaction was neglected in the BBN model, except for the 2_1^- state.

Recently, de Souza *et al.* compiled the ${}^7\text{Be}(n, p)$ reaction rate with the Bayesian R -matrix fit using all available data [14]. Since only two precise experimental results [4,12]

*iwasa@tohoku.ac.jp

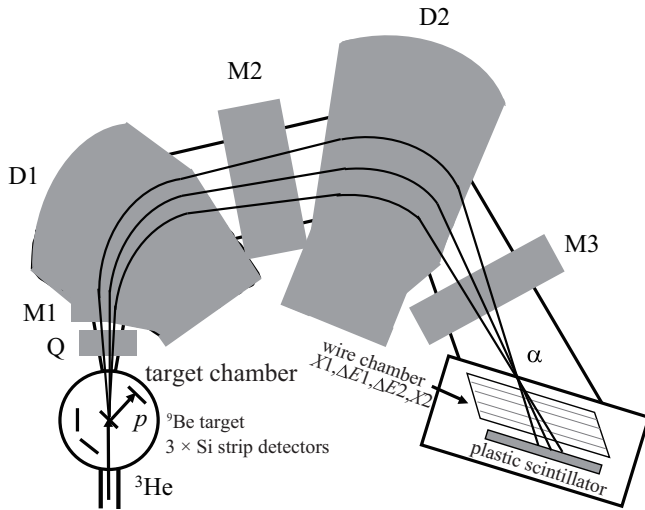


FIG. 1. Schematic view of the experimental setup.

which disagree in their absolute cross sections by 35–40% were available, the adopted reaction rate was deduced after systematical-uncertainty estimations of these experiments. The adopted rate at 0.6 GK was 2% higher than that of Descouvemont *et al.* [3] and 10% lower than that of Damone *et al.* [12]. The (n, p_1) reaction was discarded, because the $\sigma_{np1}/\sigma_{np0}$ ratios at $E_n \leq 60$ eV are smaller than the systematical uncertainties. However, it is not clear if this assumption is valid since the $\sigma_{np1}/\sigma_{np0}$ ratios at higher energies strongly depend on the properties of the resonant states, decay energy, and so on. Further experimental studies using the direct method are desired.

As an alternative method, the ${}^7\text{Be}(n, p_1){}^7\text{Li}^*$ reaction rate can be deduced when the Γ_{p1}/Γ_{p0} ratio of each resonant state is determined experimentally. In the present article, an experiment to populate resonant states from 18.9 to 20.1 MeV in ${}^8\text{Be}$ by the ${}^9\text{Be}({}^3\text{He}, \alpha){}^8\text{Be}^*$ reaction and to measure decay protons from these states into the first excited and ground states in ${}^7\text{Li}$ is reported.

II. EXPERIMENT

The experiment was carried out at the Tandem accelerator facility of Japan Atomic Energy Agency (JAEA) at Tokai. The experimental setup is shown in Fig. 1. A beryllium target with an areal density of $185 \mu\text{g}/\text{cm}^2$ was impinged by a ${}^3\text{He}$ beam at 30 MeV. The target was tilted 45° to the beam axis, resulting in an effective target thickness of $262 \mu\text{g}/\text{cm}^2$. In the target, carbon and oxygen contamination was present, corresponding to an areal density of $1.7^{+0.7}_{-0.4}$ and $2.2 \pm 0.2 \mu\text{g}/\text{cm}^2$, respectively, which were evaluated by measuring the elastic scattering of a 30-MeV ${}^4\text{He}$ beam from the AVF cyclotron at the cyclotron radioisotope center (CYRIC), Tohoku university. The α particles emitted by the ${}^9\text{Be}({}^3\text{He}, \alpha){}^8\text{Be}^*$ reaction at 0° were analyzed by the high-resolution spectrometer ENMA [15]. The horizontal and vertical angular acceptances were set to $\pm 2^\circ$ and $\pm 3^\circ$, respectively, to restrict the emission angle of residual ${}^8\text{Be}^*$. It was necessary to separate protons emitted by the decay from the

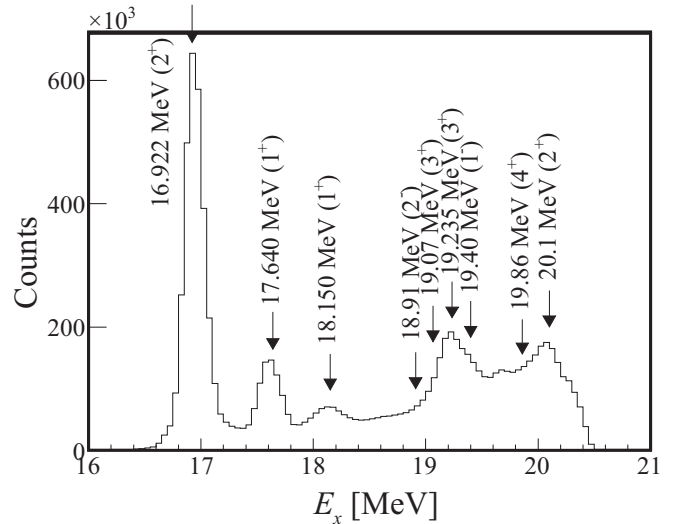


FIG. 2. Excitation energy spectrum of ${}^8\text{Be}$ populated by the ${}^9\text{Be}({}^3\text{He}, \alpha){}^8\text{Be}^*$, deduced from the magnetic rigidity of the α particles measured by ENMA. The arrows indicated to known excited states in ${}^8\text{Be}$ [16].

resonant states in ${}^8\text{Be}$ into the ground state from ones to the first excited state in ${}^7\text{Li}$. Along the focal plane of ENMA, a wire chamber and a plastic scintillator were placed. The wire chamber consists of four gas proportional counters, X1, $\Delta E1$, $\Delta E2$, and X2 operated in isobutane gas at a pressure of 150 mbar. The particle identification was performed by the ΔE - E method using the $\Delta E1$ and $\Delta E2$ counters and the plastic scintillator (E). The magnetic rigidity of the α particles was deduced from the horizontal position at the focal plane reconstructed by the tracking from the horizontal position of hit on the X1 and X2 counters measured by the charge division method.

The decay protons were measured by three silicon strip detectors with an active area of $60 \times 60 \text{ mm}^2$ with strip pitches of 5, 10, and 10 mm, respectively. They are placed at 150, 120, and 120 mm from the target at the angle (acceptance) of $59^\circ (\pm 11^\circ)$, $90^\circ (\pm 14^\circ)$, and $135^\circ (\pm 14^\circ)$, respectively. Measurements using $167\text{-}\mu\text{g}/\text{cm}^2$ -thick mylar and $100\text{-}\mu\text{g}/\text{cm}^2$ -thick carbon targets were performed for calibrating the magnetic rigidity of the α particles using the ${}^{12}\text{C}({}^3\text{He}, \alpha){}^{11}\text{C}$ and ${}^{16}\text{O}({}^3\text{He}, \alpha){}^{15}\text{O}$ reactions. These data were also used for estimating the background caused by contaminant carbon and oxygen in the beryllium target and it was found to be negligibly small.

III. RESULTS AND DISCUSSION

Figure 2 shows the excitation energy spectrum of ${}^8\text{Be}$ populated by the ${}^9\text{Be}({}^3\text{He}, \alpha){}^8\text{Be}^*$ reaction, deduced from the magnetic rigidity of the α particles. The peaks were observed at 16.9, 17.6, 18.2, 19.2, and 20.1 MeV corresponding to the 2_3^+ , 1_1^+ , 1_2^+ , 3_2^+ , and 2_4^+ states at 16.922, 17.640, 18.150, 19.235, and 20.1 MeV in ${}^8\text{Be}$ [16], respectively. The 16.922-MeV state is a state of the 2^+ doublet at 16.626 and 16.922 MeV with significant mixing of isospin $T = 0$ and 1 in their wave function. These two states were populated

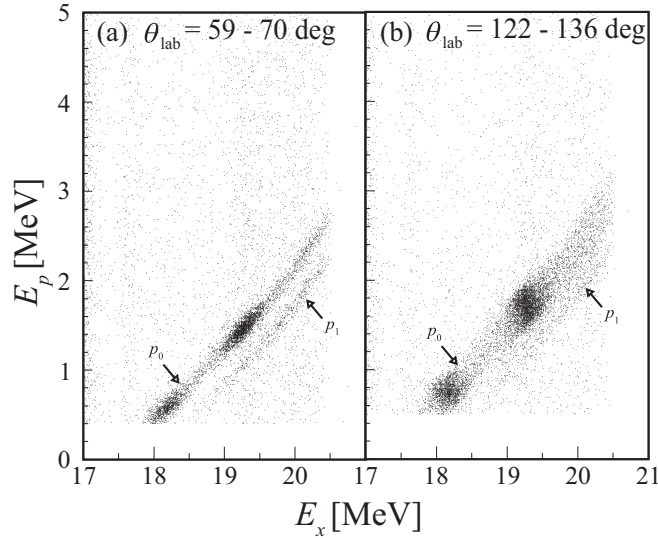


FIG. 3. Correlation of the excitation energy in ${}^8\text{Be}$ with the kinetic energy of the decay protons from ${}^8\text{Be}^*$. The upper and lower curves labeled p_0 and p_1 correspond to the decays to the ground and first excited states in ${}^7\text{Li}$, respectively.

by the ${}^7\text{Li}({}^3\text{He}, d){}^8\text{Be}$ reaction at 20 MeV and characterized by the ${}^7\text{L}(\text{g.s.})+p$ and ${}^7\text{Be}(\text{g.s.})+n$ single-particle model configurations [17]. The 1^+ doublet at 17.640 and 18.150 MeV and 3^+ doublet at 19.07 and 19.235 MeV are also considered to possess isospin mixing in their wave function [18]. The total widths of the resonant states at 16.922 and 17.640 MeV were reported to be 74.0 and 10.7 keV, respectively [16]. The resolution of the excitation energy E_x in this setup was obtained to be 80 keV in σ by fitting the peaks by the Voigt function.

The correlation of E_x with the kinetic energy of the protons at $59\text{--}70^\circ$ and $122\text{--}136^\circ$ in the laboratory frame is shown in Fig. 3. Two discrete curves were clearly observed in Figs. 3(a) and 3(b). The upper and lower curves labeled p_0 and p_1 correspond to the decays to the ground and first excited states in ${}^7\text{Li}$, respectively. The energies and angles of the protons, $E_{c.m.}$ and $\theta_{c.m.}$, and the triple differential cross section $\frac{d^3\sigma_{c.m.}}{d\Omega_\alpha d\Omega_p dE_x}$ in the rest frame of the residual ${}^8\text{Be}$ (center of mass of the ${}^7\text{Li}+p$ system) were deduced using the kinematics of the residual ${}^8\text{Be}$ calculated event by event by the kinematics.

Figure 4 shows the triple differential cross sections at $E_x = 19.15\text{--}19.25$ and $20.05\text{--}20.15$ MeV. The closed circles and open squares indicate the triple differential cross sections of the ${}^9\text{Be}({}^3\text{He}, \alpha){}^8\text{Be}^*(p_0){}^7\text{Li}$ (p_0) and ${}^9\text{Be}({}^3\text{He}, \alpha){}^8\text{Be}^*(p_1){}^7\text{Li}^*$ (p_1) reactions, respectively. The accidental coincidence events were subtracted using events whose time difference between the silicon strip detector and the plastic scintillator is 150 ns after the coincidence window (50 ns). Since the angular distributions are not isotropic, they were fit by a series of Legendre polynomials as

$$\frac{d^3\sigma_{c.m.}}{d\Omega_\alpha d\Omega_p dE_x} = \sum_{\ell=0}^{\ell_{\max}} a_\ell P_\ell(\cos \theta_{c.m.}).$$

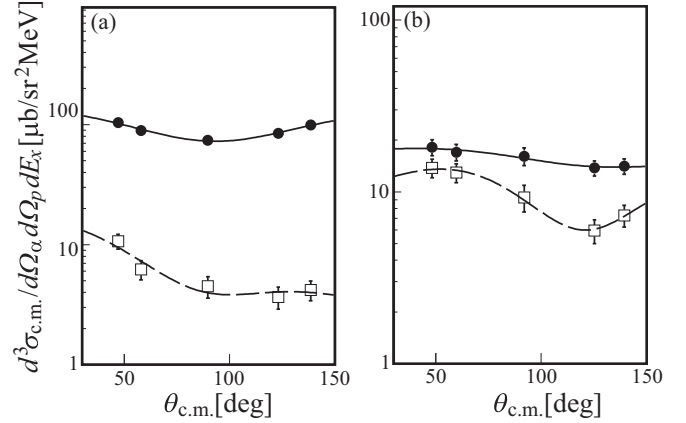


FIG. 4. Triple differential cross sections as a function of the proton emission angle in the rest frame of the residual ${}^8\text{Be}^*$ at $E_x = 19.15\text{--}19.25$ (a) and $20.05\text{--}20.15$ MeV (b). The closed circles and open squares represent the ${}^9\text{Be}({}^3\text{He}, \alpha){}^8\text{Be}^*(p_0){}^7\text{Li}$ and ${}^9\text{Be}({}^3\text{He}, \alpha){}^8\text{Be}^*(p_1){}^7\text{Li}^*$ reactions, respectively. The solid and dashed curves show the best fit results by a series of Legendre polynomials.

Since the Legendre polynomial expansion should involve a few low-order terms, $\ell_{\max} = 3$ was adopted. The solid and dashed curves in Fig. 4 show the best-fit results. The integrated double differential cross sections $\frac{d^2\sigma}{d\Omega_\alpha dE_x} = \int \sum a_\ell P_\ell d\Omega_p = 4\pi a_0$ were deduced. The systematical uncertainty of the double differential cross section due to the restriction of the ℓ_{\max} value was evaluated by using different ℓ_{\max} values and found to be less than 10% at the maximum.

The double differential cross sections of p_0 and p_1 are shown in Figs. 5(a) and 5(b), respectively. The solid curves in Fig. 5 represent the best-fit results by the sum of the single-level Breit-Wigner formalism with the Coulomb penetration of proton for seven resonant states at 18.150, 18.91, 19.07, 19.235, 19.40, 19.86, and 20.1 MeV. The E_x resolution mentioned above was taken into account. The energies and total widths of the resonant states were limited within the errors adopted in Ref. [16], and the orbital angular momentum quantum numbers in the proton emission, ℓ , were fixed to the minimum ones. As shown in Fig. 5, the 1_2^+ , 2_1^- , 3_1^+ , 3_2^+ , 4_2^+ , and 2_4^+ states at 18.150, 18.91, 19.07, 19.235, 19.86, and 20.1 MeV, respectively, in ${}^8\text{Be}$ were populated by the $({}^3\text{He}, \alpha)$ reaction. On the other hand, significant amplitude was not observed for the 1_1^- state at 19.40 MeV. Table I shows the parameters deduced by the fit. The experimental p_0 and p_1 cross sections were reproduced by the fit, except for the p_1 cross section at $E_x < 18.7$ MeV, which is lower than S_n . The branching ratio $\Gamma_{p_1}/\Gamma_{p_0}$ of the 3_2^+ state at 19.235 MeV was deduced to be $3.4 \pm 1.9\%$. The 2_4^+ state at 20.1 MeV was found to decay mainly into the ground state in ${}^7\text{Li}$, and the 1σ upper limit of $\Gamma_{p_1}/\Gamma_{p_0}$ was deduced to be 22%. On the other hand, the Γ_{p_1} of the 4_1^+ state at 19.86 MeV was observed to be larger than Γ_{p_0} , suggesting this state dominantly decays into the first excited state in ${}^7\text{Li}$. The $\Gamma_{p_1}/\Gamma_{p_0}$ ratio of the 18.91-MeV state was deduced to be $64 \pm 44\%$ which cannot reproduce the ratio of the cross section of the ${}^7\text{Be}(n, p_1){}^7\text{Li}^*$ reaction

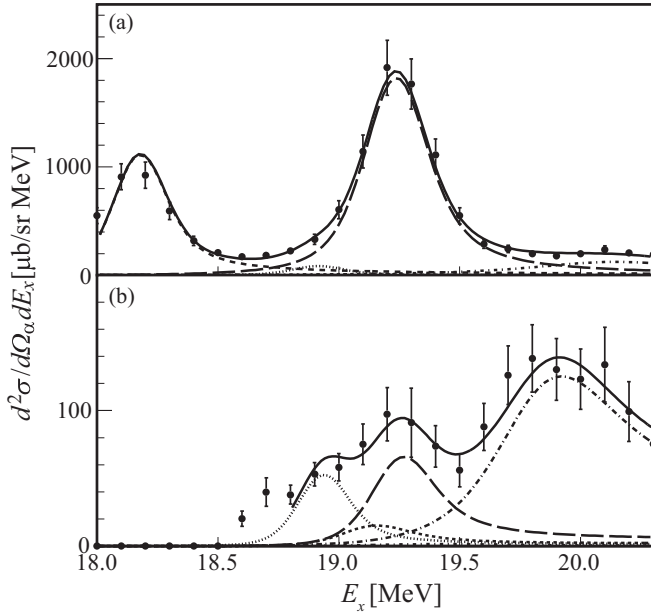


FIG. 5. Double differential cross sections of the (a) ${}^9\text{Be}({}^3\text{He}, \alpha){}^8\text{Be}^*(p_0){}^7\text{Li}$ and (b) ${}^9\text{Be}({}^3\text{He}, \alpha){}^8\text{Be}^*(p_1){}^7\text{Li}^*$ reactions. The solid curves represent the best fit results by the sum of the single-level Breit Wigner formalism with the Coulomb penetration of proton for seven resonant states at 18.150 (dashed curve), 18.91 (dotted curves), 19.07 (thick dotted curves), 19.235 (loosely dashed curves), 19.86 (dot-dashed curves), and 20.1 (thick dot-dashed curves) MeV.

to that of the ${}^7\text{Be}(n, p_0){}^7\text{Li}$ reaction measured at $E_n \leq 60$ eV [4, 13]. This discrepancy may be explained when an unknown 0^- or 1^- state predicted by shell-model calculations [19] and cluster-model calculations [20], which can be populated by the ${}^9\text{Be}({}^3\text{He}, \alpha)$ reaction and decay into the first excited state in ${}^7\text{Li}$ with $\ell = 0$, exists close to the 18.91-MeV state. Further investigations are necessary.

The resonant states at 18.91, 19.235, 19.40, and 20.1 MeV in ${}^8\text{Be}$ are considered to be important to the ${}^7\text{Be}$ destruction. Since the reaction rate through the 18.91-MeV state was determined by the direct measurements of the ${}^7\text{Be}(n, p){}^7\text{Li}$ reaction, the ${}^7\text{Be}(n, p_1){}^7\text{Li}^*$ reaction through this state was already taken into account. Figure 6 shows the ${}^7\text{Be}(n, p){}^7\text{Li}$ reaction rate. The solid curve represents the reaction rate

TABLE I. The parameters deduced by the best fit by the sum of the single-level Breit-Wigner formalism with the Coulomb penetration of protons.

J^π	E_x (MeV)	Γ (MeV)	$\frac{\Gamma_{p1}}{\Gamma_{p0}}$ (%)	$\frac{\Gamma_{p1}}{\Gamma_{p0} + \Gamma_{p1}}$ (%)
(2^-)	18.91	0.122	64 ± 44	38 ± 20
3^+	19.10	0.25		55^{+45}_{-55}
3^+	19.23	0.211	3.4 ± 1.9	3.3 ± 1.8
1^-	19.40 ^a			
4^+	19.81	0.6		100^{+0}_{-9}
2^+	20.10	0.86	0^{+22}_{-0}	0^{+22}_{-0}

^aNot populated by the $({}^3\text{He}, \alpha)$ reaction.

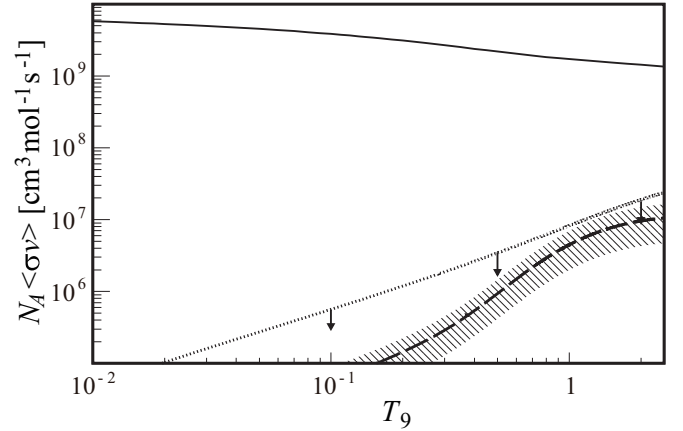


FIG. 6. Calculated ${}^7\text{Be}(n, p){}^7\text{Li}$ reaction rate. The solid curve represents the reaction rate deduced by Damone *et al.* [12]. The dashed curve shows the reaction rate of the (n, p_1) reaction through the resonant state at 19.235 MeV calculated using Γ_{p1}/Γ_{p0} deduced by the present measurement and the partial width parameters deduced by Damone *et al.* [12]. The dotted curve is the 1σ upper limit of the (n, p_1) reaction ratio through the resonant state at 20.1 MeV.

deduced by Damone *et al.* [12]. The dashed curve shows the (n, p_1) reaction rate through the 3_2^+ state at 19.235 MeV calculated using the Γ_{p1}/Γ_{p0} ratio deduced by the present measurement and the partial width parameters of Ref. [12]. The dotted curve is the 1σ upper limit of the (n, p_1) reaction rate through the 2_4^+ state at 20.1 MeV. In the BBN temperature $T_9 = 0.6$ – 1.2 , the (n, p_1) reaction rate through the 19.235-MeV state was calculated to be $0.07 \pm 0.04\%$ – $0.3 \pm 0.2\%$ of the prior ${}^7\text{Be}(n, p){}^7\text{Li}$ reaction rate [12]. The 1σ upper limit of the (n, p_1) reaction rate through the 20.1-MeV state was deduced to be 0.2–0.6% of the prior reaction rate [12].

IV. CONCLUSIONS

The resonant states at 18.91–20.1 MeV in ${}^8\text{Be}$ were populated by the ${}^9\text{Be}({}^3\text{He}, \alpha){}^8\text{Be}^*$ reaction and decay protons to the ground and first excited states in ${}^7\text{Li}$ were well-separatedly measured. The Γ_{p1}/Γ_{p0} ratio of the 19.235-MeV states was deduced to be $3.4 \pm 1.9\%$. The states at 19.86 and 20.1 MeV were found to decay dominantly into the first excited and ground states, respectively. The present result suggests the ${}^7\text{Be}(n, p_1){}^7\text{Li}^*$ reaction cross sections through the 19.235- and 20.1-MeV states are not large enough to solve the cosmological lithium problem. The (n, p_1) reaction cross section through the 19.40-MeV state cannot be determined. Further investigation using different methods is necessary to determine the Γ_{p1}/Γ_{p0} ratio of the 19.40-MeV state.

ACKNOWLEDGMENTS

The authors are grateful to the accelerator staff of the tandem accelerator facility at JAEA for their delivering the ${}^3\text{He}$ beam. The authors also thank the accelerator staff of the AVF

cyclotron at cyclotron radioisotope center at Tohoku University for their delivering beams for quantitative measurement

of contaminant in the beryllium target. The present work was supported in part by JSPS KAKENHI Grant No. JP26287058.

-
- [1] B. D. Fields, *Ann. Rev. Nucl. Part. Sci.* **61**, 47 (2011).
- [2] M. Carmona-Gallardo, B. S. Nara Singh, M. J. G. Borge, J. A. Briz, M. Cubero, B. R. Fulton *et al.*, *Phys. Rev. C* **86**, 032801(R) (2012).
- [3] P. Descouvemont, A. Adahchour, C. Angulo, A. Coc, and El. Vangioni-Flam, *At. Data Nucl. Data Tables* **88**, 203 (2004).
- [4] P. E. Koehler, C. D. Bowman, F. J. Steinkruger, D. C. Moody, G. M. Hale, J. W. Starner *et al.*, *Phys. Rev. C* **37**, 917 (1988).
- [5] J. H. Gibbons and R. L. Macklin, *Phys. Rev.* **114**, 571 (1959).
- [6] R. R. Borchers and C. H. Poppe, *Phys. Rev.* **129**, 2679 (1963).
- [7] K. K. Sekharan, H. Laumer, B. D. Kern, and F. Gabbard, *Nucl. Instrum. Methods* **133**, 253 (1976).
- [8] C. H. Poppe, J. D. Anderson, J. C. Davis, S. M. Grimes, and C. Wong, *Phys. Rev. C* **14**, 438 (1976).
- [9] R. Hanna, *Philos. Mag.* **46**, 381 (1955).
- [10] Y. M. Gledenov *et al.*, in *Proceedings of the International Conference on Neutron Physics*, Vol. 2 (Kiev, 1987), p. 232.
- [11] J. Červená *et al.*, *Czechoslovak J. Phys.* **39**, 1263 (1989).
- [12] L. Damone, M. Barbagallo, M. Mastromarco, A. Mengoni, L. Cosentino, E. Maugeri *et al.*, *Phys. Rev. Lett.* **121**, 042701 (2018).
- [13] I. Tomandl, J. Vacík, U. Köster, L. Viererbl, E. A. Maugeri, S. Heinitz *et al.*, *Phys. Rev. C* **99**, 014612 (2019).
- [14] R. S. de Souza, T. H. Kiat, A. Coc, and C. Iliadis, *Astro. Phys. J.* **894**, 134 (2020).
- [15] Y. Sugiyama, N. Shikazono, H. Ikezoe, and H. Ikegami, *Nucl. Instrum. Methods* **187**, 25 (1981).
- [16] D. R. Tilley, J. H. Kelley, J. L. Godwin, D. J. Millener, J. E. Purcell, C. G. Sheu, and H. R. Weller, *Nucl. Phys. A* **745**, 155 (2004).
- [17] A. Belhout, S. Ouichaoui, H. Beaumevielle, A. Bouchemha, G. Bogaert, S. Fortier *et al.*, *Phys. Rev. C* **96**, 054601 (2017).
- [18] J. L. Schoonover, T. Y. Li, and S. K. Mark, *Nucl. Phys. A* **176**, 567 (1971).
- [19] L. G. Arnold and R. G. Seyler, *Phys. Rev. C* **20**, 1917 (1979).
- [20] H. Stöwe and W. Zahn, *Z. Phys. A* **286**, 173 (1978).